Optical properties of the Cd_3As_2-Cd_3P_2 semiconductor alloy system*

M. Zivitz and J. R. Stevenson
School of Physics, Georgia Institute of Technology, Atlanta, Georgia 30332
(Received 26 November 1973)

The near-normal-incidence, room-temperature reflectance spectra of the Cd_3As_2-Cd_3P_2 semiconductor alloy system have been measured for photon energies $0.083 < E < 21$ eV. Synchrotron radiation has been used to extend the measurements to 30 eV for Cd_3As_2. These spectra are similar to those of III–V compounds. Comparison of the primary, reflectance data with the results of others and with the band-structure calculations has been made. The reflectance has been analyzed via the Kramers-Kronig relations. We report curves for n, k, κ_1, κ_2, and n_{eff} for all the alloys studied. Strong structure in the fundamental absorption scales approximately linearly with alloy composition. Structure at 11 eV is associated with Cd d-band excitation.

I. INTRODUCTION

Considerable attention has been given to the II–V compounds of Zn_3As_2, Zn_3P_2, Cd_3As_2, and Cd_3P_2 as a result of their interesting transport properties; for example, Cd_3As_2 is a degenerate n-type semiconductor with an exceptionally large mobility, low effective mass, and a small band gap, whereas Zn_3As_2 is a p-type semiconductor with very low mobility, a comparatively large effective mass, and a large band gap.[1-16] The practical interest in these binary semiconductors has been extended to the alloy systems Zn_3As_2-Cd_3As_2,[17,18] Cd_3As_2-Cd_3P_2,[19-22] and Cd_3As_2-Zn_3P_2.[23] Since Cd_3As_2 is an end member of each of these alloy systems, it has undergone much investigation. As found in the above references, some controversy has centered on the nature of the fundamental absorption edge in Cd_3As_2.

Numerous investigations of the band structure of groups IV, III–V, and II–VI binary compounds (and their alloys) have been conducted by means of the analysis of their reflectance spectra. The interpretation of the results is facilitated whenever tentative band-structure calculations have been available.[24] Band-structure calculations[25,26] have recently been performed for several II–V compounds. As little research has been performed on these alloys beyond the fundamental absorption edge,[27-30] the interpretation of our results has been aided by comparison with the above band-structure calculations and with some of the work on III–V semiconductors.

We have measured the near-normal-incidence reflectance spectra of these II–V alloys over a very large range (0.08–30 eV) of photon energy. The high-energy limit of our measurements was extended by use of ultraviolet radiation from the electron storage ring at the University of Wisconsin Physical Sciences Laboratory.[31] A Kramers-Kronig analysis was used to generate the optical constants, and we have compared results with the limited (spectrally speaking) results of others.[8,10,27,29] An assignment of a number of interband transitions has been made, and these transitions have been located as a function of alloy composition. Qualitative agreement has been obtained with the available band-structure calculations.

A brief discussion of the chemical considerations and the current band-structure calculations is presented in Sec. II. The experimental techniques are presented in Sec. III and the primary results are given in Sec. IV. Also included in Sec. IV is a discussion of the reflectance structure above 0.7 eV. Section V presents the optical constants and our interpretation of the transitions which underlie the fundamental absorption edge.

II. THEORETICAL CONSIDERATIONS

The II–V compounds Cd_3As_2 and Cd_3P_2 belong to the tetragonal crystal system. The space group for Cd_3As_2 is $I4_1cd$[32,33] and that for Cd_3P_2 is $P4_2/nmc$.[5,34] The unit cell for Cd_3As_2 is composed of 32 formula units, and the unit cell for Cd_3P_2 is composed of eight formula units. On the basis of Masumoto's x-ray work[2] and a discussion of the polymorphic transformation[32] in the related Cd_3As_2-Zn_3As_2 alloy system, we find that two Cd_3P_2 unit cells[33] can be inscribed within the Cd_3As_2 unit cell.[34] (The basal vectors are related by a factor $\sqrt{2}$; the c axes by a factor 2.)

The coordination of ions is similar in this and in the Cd_3As_2-Zn_3As_2 alloy system. In Cd_3As_2 the large As ions are cubic close-packed, and three-fourths of the tetrahedral interstices are occupied by Cd ions (note that vacancies exist in the ideal crystal structure). Each As ion is surrounded by Cd ions at six of the eight corners of a cube. The relative disposition of these vacancies differen-

tiates the unit cells of the arsenides from those of the phosphides. If one envisages a lattice of arrows connecting adjacent pairs of these vacant sites, then the repeat distance along the c axis of the pattern of arrows differs for the arsenides and the phosphides.

Although Cd_3As_2 and Cd_3P_2 possess slightly different crystal structures, the more important features of their electronic structures seem related to their similar chemical composition. The Cd and Zn atoms have an outer filled s shell, an empty p shell, and a filled d shell about 9 eV below the filled s shell. The As and P atoms have a filled s shell and three electrons in their outer p shell. No other electrons lie at energies accessible to our measurements. Table I lists the ionization energies,[35] referred to vacuum, of the neutral atomic components of the alloys investigated. The $4d$ level at 17.6 eV for Cd has been obtained from the multiplicity-weighted average of the $^2D_{3/2}$ and $^2D_{5/2}$ terms given by Harrison.[36] A first approximation to the separation of the d band and valence band in the solid is given by the difference between the d shell in the group-II B atom and p shell of the group-V atom.

The above approximation ignores the energy shift caused by a transfer of charge in the more ionic crystals. In the event of such a shift, one should more appropriately use the first ionization energies of the stripped atoms.[37] Suchet[38] has formulated an empirical, electronegativity theory from which the homopolar $\mathcal{E}_1$ and heteropolar $\mathcal{E}_2$ contributions to the fundamental energy gap, $\mathcal{E}_g = \mathcal{E}_1 + \mathcal{E}_2$, have been computed for a large number of semiconducting, binary compounds. We define the fraction f_i of ionic character as $f_i \equiv \mathcal{E}_2/\mathcal{E}_g$. For Cd_3As_2, f_i is found to be on the order of 1.0 while a value of 0.8 is found for Cd_3P_2.

Lin-Chung[25,26] has performed pseudopotential calculations for the energy-band structures of Cd_3As_2, Zn_3As_2, Cd_3P_2, and Zn_3P_2. The crystal structure has been simplified by filling all the vacancies. For example, in Cd_3As_2 the vacancies are filled with Cd ions. This hypothetical unit cell then transforms into 16 fluorite unit cells with As^{3-} replacing the Ca^{2+} and the Cd^{2+} replacing F^- in the calcium-fluoride structure. The Brillouin zone for this fluorite structure is much larger than that for either Cd_3As_2 or Cd_3P_2 and is identical to that of the fcc structure. The high symmetry points[39] of this fluorite structure are also symmetry points of the real Brillouin zone. Figure 1 demonstrates these two Brillouin zones. The Brillouin zone for the fcc structure is 16 times larger than that for Cd_3As_2 and four times larger than that for Cd_3P_2 (this follows since the real unit cells of Cd_3As_2 and Cd_3P_2 have a direct volume ratio of four-to-one). An effective vacancy pseudopotential is incorporated into the Cd atomic pseudopotential to account for the presence of the vacancies.

There is a strong similarity between the over-all calculated energy-band structures of Cd_3As_2 and Cd_3P_2, and both resemble those of the III–V compounds (InAs, GaSb, etc.). Some experimental justification is present for these structure approximations, since the optical spectra to be given later are similar to those of III–V compounds. Figure 2 gives the energy-band structures for Cd_3As_2 and Cd_3P_2 as calculated by Lin-Chung. The

TABLE I. Ionization energies of the neutral atomic components of the alloys investigated.

II		V	
Zn	Cd	P	As
$4s$	$5s$	$3p$	$4p$
9.38 eV	8.99 eV	9.79 eV	9.24 eV
$3d$	$4d$	$3s$	$4s$
17.40 eV	17.60 eV	18.35 eV	17.67 eV

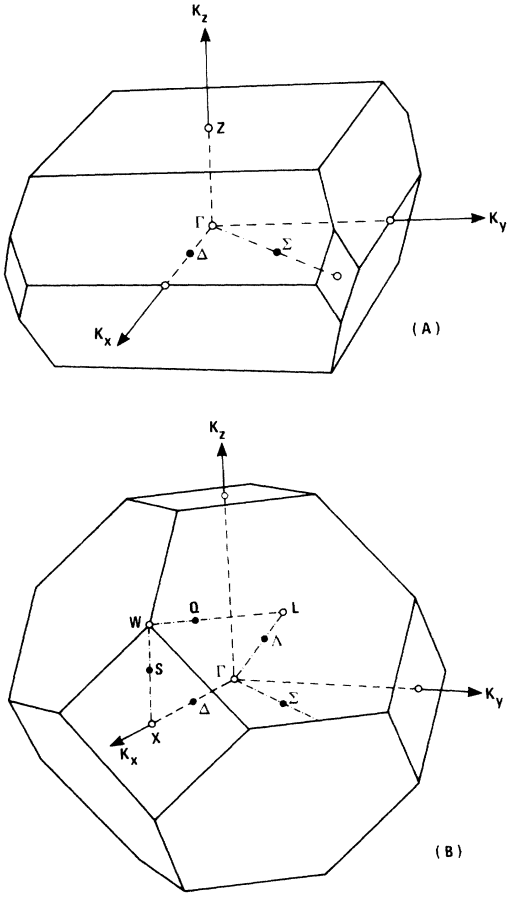

FIG. 1. First Brillouin zone of (a) body-centered tetragonal structure and (b) fluorite structure.

lowest valence band is an anion s-like level; the second valence band is a Cd s-like level; and the third and fourth are s-like about Cd and p-like about the anion. The valence-band maximum for Cd_3P_2 is at Γ; that for Cd_2As_2, slightly (~12%) off-center of the Brillouin zone. The bottom of the conduction band at Γ has an s-like representation Γ_1. The predicted energy gap for Cd_3As_2 is ~0.2 eV or smaller.

III. MEASUREMENTS

The energy range 0.083–30 eV required the use of four optical systems. The description of these systems has been reported in detail.[40] The region $0.083 < E < 1.9$ eV (1.5–0.65 μm) was investigated by using a Perkin-Elmer Corporation "Optical Reflectance Attachment" and a Perkin-Elmer model 99 monochromator with a NaCl prism. Both a globar and tungsten-halogen lamp were used as sources, and a Reeder Corporation thermocouple was used with a synchronous-rectification detection scheme. The reflectance measurements were taken at room temperature and atmospheric pressure.

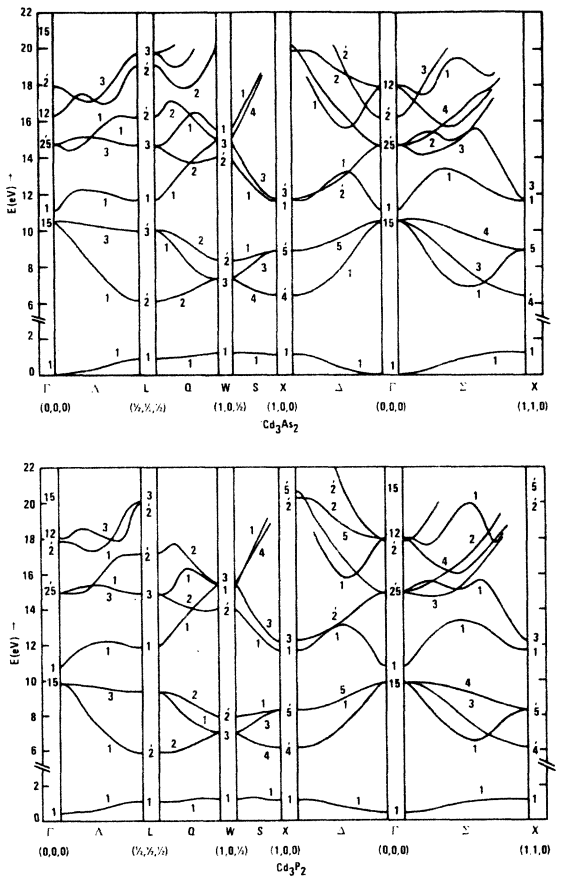

FIG. 2. Energy band structures for Cd_3As_2 and Cd_3P_2 compounds as calculated in the hypothetical structure.

From 1.9 to 7.3 eV (6500–1700 Å) the sample chamber was constructed from an ultrahigh-vacuum (10^{-8} Torr) system of conventional design and was provided with an ion pump. A McPherson 0.3-m scanning monochromator with provisions for evacuation and easy interchange of gratings (1500-Å and 5000-Å blaze angles) served to span this range. A lithium-fluoride window flange was used to support the pressure differential between the reflectometer and monochromator. Both a tungsten-halogen lamp and a glow discharge in several Torr of hydrogen provided continuum sources in this range. A 13-stage photomultiplier (PM) tube and light pipe (phosphor coated above 3 eV) served as the base for simple dc detection.

The region from 7.3 to 21 eV (1700 to 600 Å) was investigated by means of a General Electric GEI-44854, 1-m normal-incidence monochromator, similar to that designed by Johnson.[41] This monochromator was provided with an 800-Å blazed grating, and the sample chamber used by Hinson[42] was employed. A 13-stage PM tube was used with a sodium-salicylate-coated light pipe and synchronous-rectification detection schemes. Below 13 eV, a glow-discharge lamp was operated in a dc mode to provide the many-lined hydrogen spectrum. A tuning-fork chopper interrupted the emergent beam from the monochromator and provided a reference signal. Above 13 eV, the glow-discharge lamp was operated in a repetitive, condensed discharge mode to provide the Hopfield continuum. The ac line to a McPherson 720 spark supply was interrupted to generate a 30-Hz fundamental in the radiation which reached the PM tube.

Synchrotron radiation from the 240-MeV electron storage ring at the University of Wisconsin's Physical Sciences Laboratory provided an intense continuum which extended the high energy of our data to 30 eV. A simple reflectometer, employing a channel-electron multiplier in a current-integrated mode, was attached to the exit-slit housing of a 1-m, normal-incidence monochromator. Repeated scans were employed for the "sample-in" and "sample-out" configurations. The count rates were normalized to the electron-beam currents.

A total of eight samples were obtained from the Naval Research Laboratory (NRL) of Washington, D. C. All the members $Cd_3(As_xP_{1-x})_2$, where $0 < x \leq 1$, were prepared by a modified Bridgman method.[43] Our observations, as well as those of Wagner *et al.*,[20] were that the $Cd_3(As_{0.25}P_{0.75})_2$ and the $Cd_3(As_{0.12}P_{0.88})_2$ crystals are not mechanically strong. Radoff and Bishop[22] have reported that for $x = 0.25$ the Bridgman-grown ingots show cracks associated with a solid-solid phase transition.[19]

Mechanical polishing and etching techniques were

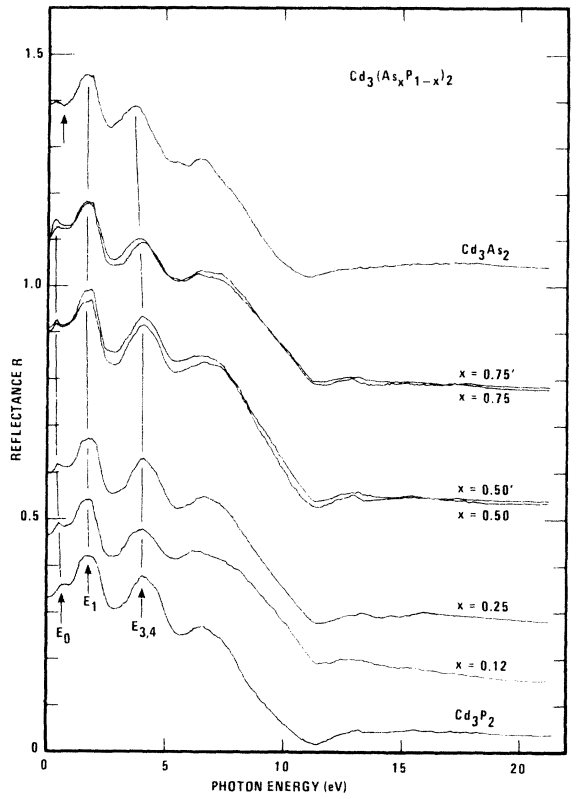

FIG. 3. Reflectance spectra of the $Cd_3(As_xP_{1-x})_2$ alloy system at 297 °K (the curves are zero shifted as explained in the text).

developed along lines suggested by the group at NRL.[44] Polishing began with a mixture of 1-μm alumina powder (Union Carbide) and tap water, and was continued until no scratches were visible except those left by the powder. This was followed by polishing with a suspension of $\frac{1}{4}$-μm diamond compound (Buehler *AB* Metadi) in a lapping oil (Buehler *AB* Automet). Final polishing was performed with a mixture of 0.05-μm (500-Å) alumina powder and distilled water. Only limited success was obtained with an etch consisting of a solution of bromine in methanol (5%–0.08% by volume). Little effort was expended toward orientation of the crystallographic axes. Although cracked, the crystalline regions of several of the samples were sizable.

IV. RESULTS AND TRENDS ABOVE 0.7 EV

The results of the near-normal-incidence reflectance measurements are presented in Fig. 3. These curves are zero shifted in relation to the percentage of the anion concentration. For several typical results, the nearly transparent or plasmon region is also shown in Fig. 4. The results of the extreme-uv measurements are presented in Fig. 5. Included in this latter figure are the results of measurements on the related compound Zn_3As_2.[25] We note that the structure in the reflectance curves of the mid-members of this alloy system is as well defined as that for the end-members.

We defer treatment of the sharp structure below 0.7 eV in Fig. 3 and begin with a discussion of the structure in the range of 2 eV. Figure 3 suggests a linear scaling of the position of this peak versus the alloy composition. In accordance with the work of Sobolev *et al.*[29] on Cd_3As_2, we label this peak E_1. The more refined data of Sobolev has shown this peak to be split by ~0.2 eV (see Fig. 6). The center of gravity of our peak for Cd_3As_2 agrees well with Lin-Chung's band-structure (BS) calculation. The corresponding peak for Cd_3P_2 agrees poorly with the respective BS calculation. See Table II for a comparison of these observed

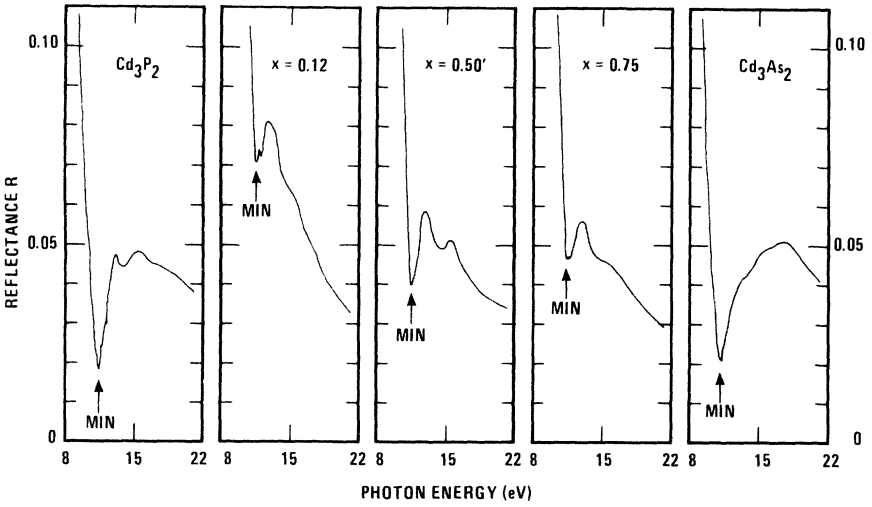

FIG. 4. Reflectance spectra of the $Cd_3(As_xP_{1-x})_2$ alloy system in the plasmon region.

peaks with the BS calculations. The probable assignments are made by analogy to the zinc-blende III–V compounds (e.g., GaAs).

The doublet character of this peak in Cd_3As_2 is presumably due to the spin-orbit splitting of the upper valence band (Λ_3) along the Λ direction. This upper valence band is p-like about the As atoms. A good estimate of the spin-orbit splitting[45-47] of the upper valence band at the Γ point can be obtained from the spin-orbit splitting of the states of p character of the isolated anion atom (e.g., the terms $^2P_{1/2}$ and $^2P_{3/2}$ of As III). In going from the isolated anion atom to the solid, the splitting is enhanced by the factor $\frac{29}{20}$. Using Moore's tabulation[37] of atomic terms, we thereby obtain 0.1 and 0.53 eV for the spin-orbit splitting at Γ in Cd_3P_2 and Cd_3As_2, respectively.

In analogy to the III–V compounds, the splitting observed in the reflectance structure is along the Λ direction. Along this direction the upper valence band is, presumably, further spin-orbit split. The degree of the latter splitting is $\frac{2}{3}$ of the splitting at the Γ point.

We therefore expect the observed splitting of the reflectance peak in the range of 2 eV to be 0.067 and 0.35 for Cd_3P_2 and Cd_3As_2, respectively. This estimate of 0.35 eV is in qualitative agreement with the 0.2-eV splitting observed by Sobolev. The resolution of our instrumentation in this region has prevented our observation of this splitting in Cd_3As_2. However, our estimated splitting of 0.067 eV for Cd_3P_2 would surely be obscured by lifetime broadening at room temperature. It is clear that the contribution to the "joint density of states" is large along a range of the line from Γ to L, since the bands Λ_1 and Λ_3 are nearly parallel in both Cd_3As_2 and Cd_3P_2 near the L point.

The peak in the range of 4 eV is labeled $E_{3,4}$, since it corresponds to an average of the locations of the peaks E_3 and E_4 found by Sobolev in Cd_3As_2 (see Fig. 6). In both end-members of this alloy system we assume that the peak E_3 corresponds to the transition $X_5' \rightarrow X_3$ and that E_4 corresponds to $\Lambda_3 \rightarrow \Lambda_1$. In Cd_3P_2, the nearby transition $\Gamma_{15} \rightarrow \Gamma_{25}$ appears to be as likely an assignment as $\Lambda_3 \rightarrow \Lambda_1$ for peak E_4. The peak E_2 is not resolved in our data. We assume that peak $E_{3,4}$ scales with the composition as shown in Fig. 3. If the peak $E_{3,4}$ indeed scales as illustrated, then our results are in qualitative agreement with the BS calculations (see Table II).

The structure of this peak $E_{3,4}$ represents a departure from the corresponding structure in the III–V compounds. In GaAs the similar peak, which is located around 5 eV, is associated with the transition $X_5 \rightarrow X_1$. A slightly higher-energy (~0.5 eV) satellite is identified with $X_5 \rightarrow X_3$ and

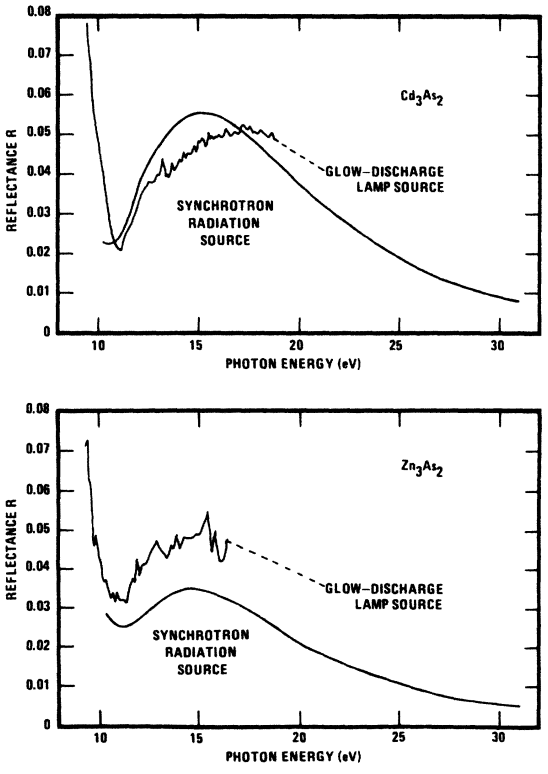

FIG. 5. Reflectance spectra of Cd_3As_2 and Zn_3As_2.

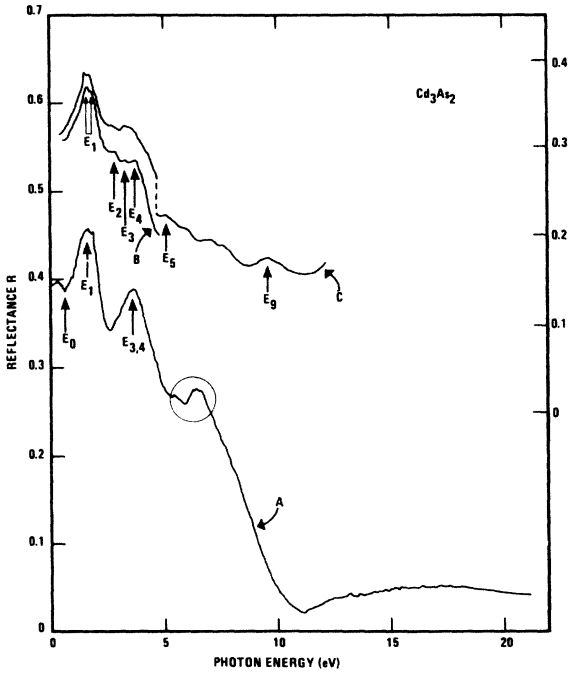

FIG. 6. Relation of (A) the present results to (B) the 77 °K data and to (C) the 293 °K data of Ref. 29 (the upper curves are zero shifted).

a lower-energy (~0.5 eV) energy shoulder is identified with $\Gamma_{15} \rightarrow \Gamma_{15}$ transitions. (The above representations belong to GaAs.[48]) In contrast to this distribution of oscillator strengths in GaAs, we associate vanishingly small oscillator strength in the II–V alloys with the $X_5' \rightarrow X_1$ transition. The BS calculations predict $X_5' \rightarrow X_1$ to be at 3.4 eV and 2.7 eV in Cd_3P_2 and Cd_3As_2, respectively. The assignments $\Lambda_3 \rightarrow \Lambda_1$ for a contribution to the peak $E_{3,4}$ are nearly zone centered, and thus correspond to $\Gamma_{15} \rightarrow \Gamma_{15}$ in GaAs. However, in the Cd_3As_2-Cd_3P_2 system, the transition $\Lambda_3 \rightarrow \Lambda_1$ lies above $X_5' \rightarrow X_3$ (at least in Cd_3As_2), and in GaAs the transition $\Gamma_{15} \rightarrow \Gamma_{15}$ lies below $X_5 \rightarrow X_1$.

The decrease in reflectance between peak $E_{3,4}$ and the rise at 11 eV is similar to that found in III–V compounds and corresponds to the near exhaustion of the f-sum rule for interband transitions.[49] This over-all decrease in reflectance typically signals the onset of the plasmon region. Below, we shall find a broad peak in the characteristic-energy-loss function in the range of 9.5 eV for all members of this alloy system.

Figure 4 shows that all samples exhibit a sharp increase in the reflectance at ~11 eV. Since the bonding in these alloys appears to have a large ionic character, it is reasonable to assume that the Cd 4d atomic levels generate a narrow band below the valence bands (in a tight-binding picture, charge transfer will lower these levels in the solid). This consideration of the relative position of the d band is these alloys and the fact that this onset at 11 eV is independent of alloy composition lead us to the conjecture that this threshold corresponds to the onset of "real" d band-to-conduction-band transitions. The data obtained for Cd_3As_2 and Zn_3As_2 at the electron storage ring provide evidence that this structure at 11 eV is not due to an instrumental error (see Fig. 5).

TABLE II. Probable assignments, between 0.7 and 6 eV, of interband transitions.

Reference No. 29	Peaks	Cd_3As_2 293°K	77°K	B.S. calculation	Probable location
	E_1	1.7	1.74	1.7	$\Lambda_3 \rightarrow \Lambda_1$
	E_1'	1.88	1.90		$\Lambda_3 \rightarrow \Lambda_1$
	E_2	2.86	2.86	2.7	$\Sigma_4 \rightarrow \Sigma_1$
	E_3	3.33	3.26	2.8	$X_5' \rightarrow X_3$
	E_4	3.7	3.7	3.9	$\Lambda_3 \rightarrow \Lambda_1$
	E_5	5.15	...	4.7	$\Lambda_3 \rightarrow \Lambda_3$
				5.2	$X_4' \rightarrow X_1$

Present results	Peaks	Cd_3As_2 297 °K	B.S. calculation	Probable location
	E_1	1.7	1.7	$\Lambda_3 \rightarrow \Lambda_1$
	$E_{3,4}$	3.6	2.8	$X_5' \rightarrow X_3$
			3.9	$\Lambda_3 \rightarrow \Lambda_1$

Present results	Peaks	Cd_3P_2 297 °K	B.S. calculation	Probable location
	E_1	1.9	2.4	$\Lambda_3 \rightarrow \Lambda_1$
	$E_{3,4}$	4.0	3.9	$X_5' \rightarrow X_3$
			5.1	$\Lambda_3 \rightarrow \Lambda_1$

In the ionic II–VI compounds CdS, CdSe, and CdTe Freeouf[50] has identified a doublet at ~13.5 eV with the spin-orbit-split transition from the Cd 4d level. In contrast, rudimentary measurements[51] on elemental Cd have revealed no semblance of structure in this spectral region.

Since we have thus far chosen to interpret the reflectance structure directly and since there exists no values of the optical constants beyond the fundamental edge, we find it convenient to compare our reflectance values with the results of others at this stage of the exposition. A detailed account has been reported.[40] We merely note here that the apparent tiny structure beyond the point labeled "MIN" in Fig. 4 is due to a systematic error.

Both Turner *et al.*[3] and Haidemenakis *et al.*[8] have reported infrared, plasma-edge, reflectance measurements for Cd_3As_2. These measurements overlap our low-energy reflectance spectra and provide a check on our absolute values. We obtain better agreement with Ref. 3 and the percentage difference of the present results with respect to those of Turner *et al.* is +8% at 0.25 eV. Since both Refs. 3 and 14 located the ir plasma edge at ~0.05 eV, we shall subsequently define the optical dielectric constant to be that dielectric constant between the fundamental absorption edge and the Restrahlen bands or the ir plasma edge. We find that this definition is compatible with the optical properties of Cd_3As_2, since the photon-energy interval between the plasma edge and the fundamental edge (~0.6 eV) is so large.

At higher photon energy we compare our reflectance values for the end member Cd_3As_2 with those of Sobolev *et al.*[29] in Fig. 6. The curves labeled "B" and "C" are equally zero shifted as indicated to prevent overlap. The measurements of Sobolev have been performed on single, unoriented crystals. His 293°K data are discontinuous not only in absolute magnitude, but also in shape. (Our data suffered background problems in the encircled region of this figure.) At 1.6 eV our data have an absolute error of +12% with respect to the data of Sobolev. In view of our error analysis,[40] we believe the data of Sobolev are not well disposed to an absolute scale.

When the data of Fig. 6 are inspected more closely, it is seen that our structure is poorly defined relative to that of Sobolev. We can only assume that this lack of definition is due to the poor crystalline quality or that the damaged layer

incurred during the mechanical polishing has not been removed by the etchant. Between 5 and 12 eV, Sobolev also obtained a series of peaks labeled E_5–E_9.

Sobolev *et al.*[27] has also performed rudimentary, reflectance measurements on Cd_3P_2. Figure 7 displays the present results for Cd_3P_2 and those of Sobolev, whose curve is given in arbitrary units. Their peak at ~4 eV is reasonable in view of our results. Note the strong similarity of this peak in our results for all members of this alloy system in Fig. 3. The fact that Sobolev has used a polycrystalline sample of Cd_3P_2 leads us to believe that the departure of our results from those (on single crystals) of Sobolev in Fig. 6 is attributable to a polycrystalline surface of our prepared samples. The remaining portion of their data on Cd_3P_2 does not seem reasonable.

V. OPTICAL CONSTANTS

Since the present results are representative of a polycrystalline surface, we have used the simple expressions

$$n = (1 - |\tilde{r}|^2)/(1 - 2|\tilde{r}|\cos\theta + |\tilde{r}|^2), \tag{1}$$

$$k = 2|\tilde{r}|\sin\theta/(1 - 2|\tilde{r}|\cos\theta + |\tilde{r}|^2), \tag{2}$$

for the real and imaginary components of the complex index of refraction

$$\tilde{N} = n + ik. \tag{3}$$

The reflectivity is defined via

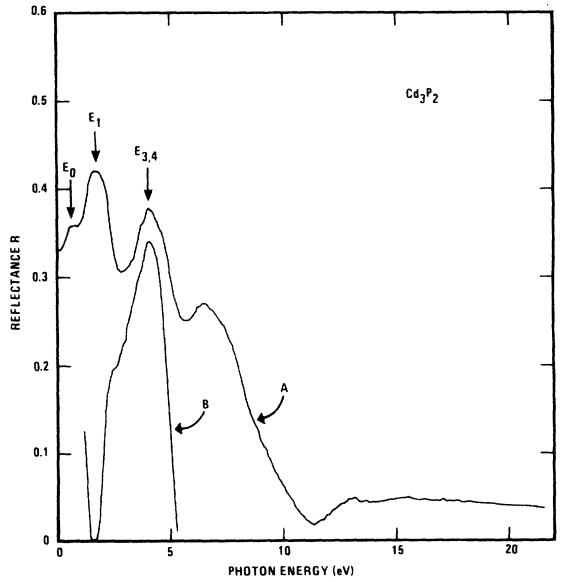

FIG. 7. Relation of (A) the present results to (B) the 293 °K data of Ref. 27 (the lower curve is given in arbitrary units).

$$\tilde{r} = |\tilde{r}|e^{i\theta}, \quad 0 \leq \theta < \pi \tag{4}$$

so that the phase shift θ is that of the magnetic field.[40,52] We have integrated the Kramers-Kronig integral

$$\theta(E) = (-1/2\pi)P\int_0^\infty \left(\frac{d\ln R(E')}{dE'}\right)\ln\left|\frac{E'+E}{E'-E}\right| dE' \tag{5}$$

by choosing the upper-energy limit of the integral, so that the phase shift vanishes below the fundamental band gap.

Our assumed form for the reflectance ($R \equiv |\tilde{r}|^2$) above 21 eV is not completely arbitrary. If indeed the absorption above 11 eV is due to the Cd 4*d* levels, then the reflectance curve of Fig. 5 for Cd_3As_2 provides an "assumed" form for all members of this alloy system. That portion of the reflectance data below the adjusted upper limit has been numerically integrated by means of a computer program kindly furnished by Shay.[53] The gap energies at which the phase shifts vanish are the room-temperature gaps reported by Wagner *et al.*[20]

We present the results of the phase-shift analysis in the form of curves for the dual quantities n and k. These curves are given in Fig. 8. The zero shifting for either family of curves is in the successive amount of one unit.

At 0.4 eV, we obtain the value of $n = 4.04$ for Cd_3As_2. In this same region, Haidemenakis *et al.*[8] obtained the estimate $n = 4.3$ ($n_\infty = \kappa_\infty^{1/2}$). Zdanowicz[10] found $n = 5$ and $k = 0.04$ ($k = c\alpha/2\omega$) at 0.413 eV (3 μm). These latter values of n and k yield a normal-incidence reflectance of 0.44 [$\tilde{r} = (\tilde{N}-1)/(\tilde{N}+1)$], which is even 10% greater than our value. Recall that our reflectance was greater than that of both Refs. 3 and 8. Of greater significance is the fact that both these other results lead to an energy dependence of n (and R) opposite ours in this low-energy region. The cause of the disagreement is not apparent.

Zdanowicz has found a sharp peak in n at ~0.6 eV. This peak has been associated[10,25] with the fundamental absorption edge in Cd_3As_2. The underlying transition is thought to be zone centered in the real crystal structure ($\Gamma_{15} \rightarrow \Gamma_1$). Our Cd_3As_2 data exhibit only a weak shoulder in n at ~0.6 eV.

Now use is made of the relations

$$\kappa_1 = n^2 - k^2 \tag{6}$$

and

$$\kappa_2 = 2nk \tag{7}$$

which yield the real and imaginary components of the complex dielectric constant (relative permittivity)

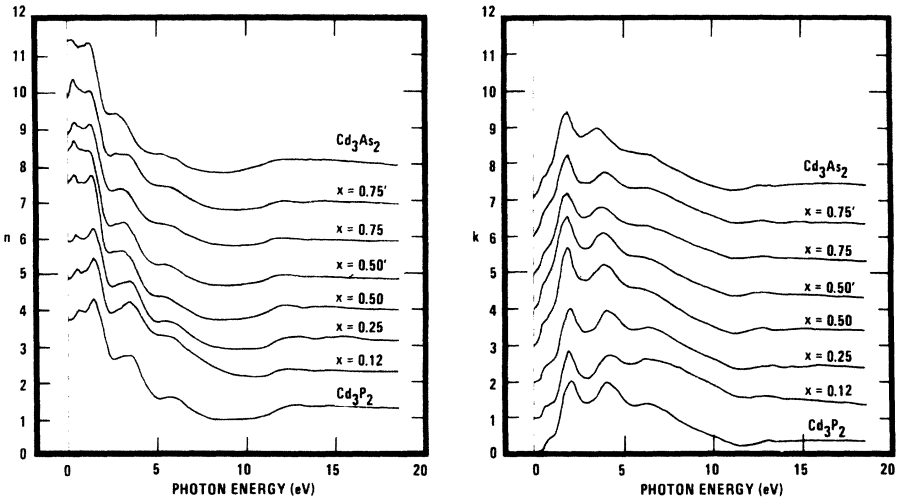

FIG. 8. Optical constants n and k for the $Cd_3(As_x P_{1-x})_2$ alloy system (the curves are successively zero shifted in the amount of one unit).

$$\tilde{K} = \kappa_1 + i\kappa_2. \tag{8}$$

The families of these quantities are given in Fig. 9. As usual, the structure in the κ_2 curve is seen to follow that in the reflectance.

We now turn our attention to the structure below 0.7 eV. The structure in this particular region is sufficiently well-defined as to be amenable to a description in terms of the joint density of states.

Several characteristic shapes in κ_2 resemble four basic forms ($M_0 - M_4$) of the joint density of states in the range of allowed transitions at critical points which are also symmetry points.[24] Representative structure in κ_1 and κ_2, along with the reflectance R is illustrated in Fig. 10. (True critical-point line shapes are rarely found in such spectra; however, they serve as a useful guide to line-shape analysis).

With the exception of Cd_3As_2, we have marked two discontinuities in the slopes of the κ_2 curves. The solid arrow locates what appears to be an M_0 critical point; the dotted arrow, an M_1 critical point. In the case of Cd_3As_2, the arrow appears to locate an M_0 critical point; however, we have encountered large relative error in this spectral region.

We have been aided in the determination of the location of the M_0 critical points by the room-temperature gaps of Wagner *et al.*[20] The underlying transition is $\Gamma_{15} \rightarrow \Gamma_1$, according to Lin-Chung's BS calculations. Figure 11 gives a plot of the location of this M_0 critical point as a function of alloy composition. Note the agreement with the transmission edges found by Ref. 20.

These critical-point identifications have been made in the following way. The sharp rise in the κ_2 curves at the point labeled by the solid arrow is characteristic of an M_0 critical point.[54] Were this the only nearby contribution to the joint density of states, one would further expect κ_1 (and R,

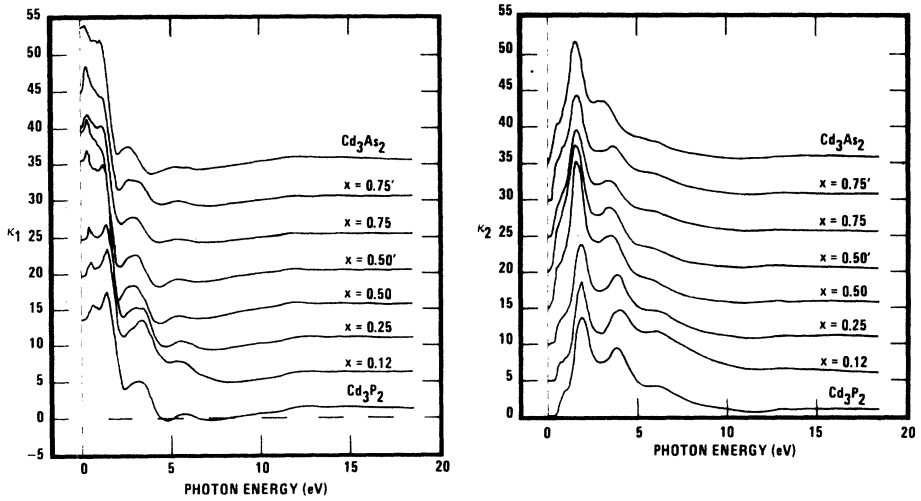

FIG. 9. Dielectric constants κ_1 and κ_2 for the $Cd_3(As_x P_{1-x})_2$ alloy system (the curves are successively zero shifted in the amount of five units).

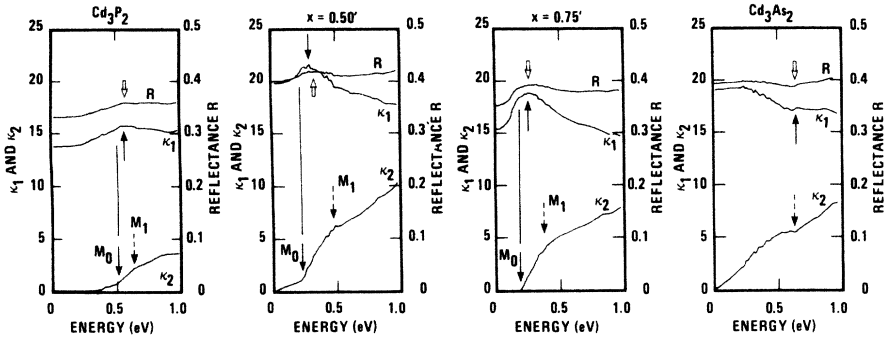

FIG. 10. Dielectric constants for typical samples.

since k is small here) to peak at the same location. We observe that in all cases, except for Cd_3As_2, the κ_1 curve peaks above the location of the M_0 critical point. An explanation of this relative shift in structure is readily obtained if the change in slope of the κ_2 curves (located by the dotted lines) is due to an M_1 critical point. An M_1 critical point gives rise to peaking of the κ_1 curve slightly below the location of the M_1 critical point.[55] Thus, we find that the interpretation of two nearby critical points, M_0 and M_1, contributing to a peaking of κ_1 (and R) between the location of these critical points is consistent with the dielectric constants.

The location of the M_1 critical point is in qualitative agreement with Lin-Chung's BS calculations. The X point and the Γ point of the hypothetical structures are equivalent in the real crystal structure: the X point becomes a Γ point. We, therefore, envisage the direct transitions in the real structure giving rise to the M_1 critical point to be $\Gamma_{15} \rightarrow X_1$ in these alloys. We are unable to identify the exact type of critical point in Cd_3As_2, but we assume the same transition is involved. Lin-Chung has placed this transition $\Gamma_{15} \rightarrow X_1$ at 1.2 eV in Cd_3As_2, and believes that it corresponds to the direct gap $\mathcal{E}_g$ found by Zdanowicz[10] at ~0.6 eV. In Cd_3P_2, she has placed the transition $\Gamma_{15} \rightarrow X_1$ at 1.875 eV. We find this transition at ~0.63 eV in Cd_3P_2, and therefore have the same qualitative agreement with the BS calculations as did Zdanowicz for Cd_3As_2. Figure 11 also displays the composition dependence of this M_1 critical point and includes the low-temperature gaps given by Radoff and Bishop.[22]

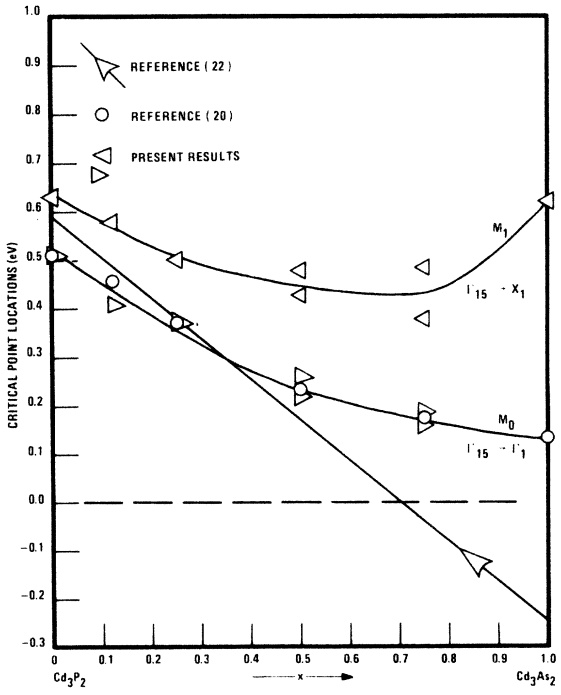

FIG. 11. Location of the band-edge critical points as determined by the structure in κ_2.

Error estimates for the dielectric constants have been discussed elsewhere.[40] We report here that the optical dielectric constants have probable errors of ±18%. In view of the above comparisons of our primary data with that of others, the optical constants at higher energy are only qualitatively correct.

The expression ("partial" sum rule)

$$n_{\text{eff}} = [2m/N(he)^2] \int_0^E E' \kappa_2(E')\, dE', \tag{9}$$

yields an effective number of free electrons contributing to the optical properties over a finite range $0 < E' < E$. N is the atomic density of the solid. The successive values of n_{eff} are displayed in Fig. 12. Since there are exactly 3.2 valence electrons per atom, we are somewhat surprised to find that these curves nearly saturate (before the rise at 12 eV) at a value of ~2.2. In particular, since the Cd d-band transitions are expected to overlap nearly the tail of the fundamental absorption spectra in these alloys, we should look for an enhancement of n_{eff} over the valence-electron contribution of 3.2. We attribute this disagreement to absolute reflectance values which are low above ~6 eV. Sample $x = 0.12$ appears to represent a favorable counter example to the failure of n_{eff}

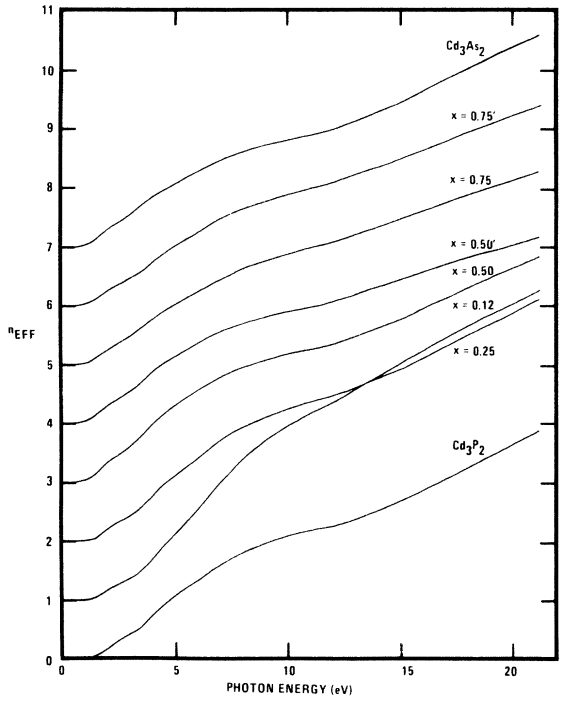

FIG. 12. Successive contributions to n_{eff} (the curves are repeatedly zero shifted in the amount of one unit).

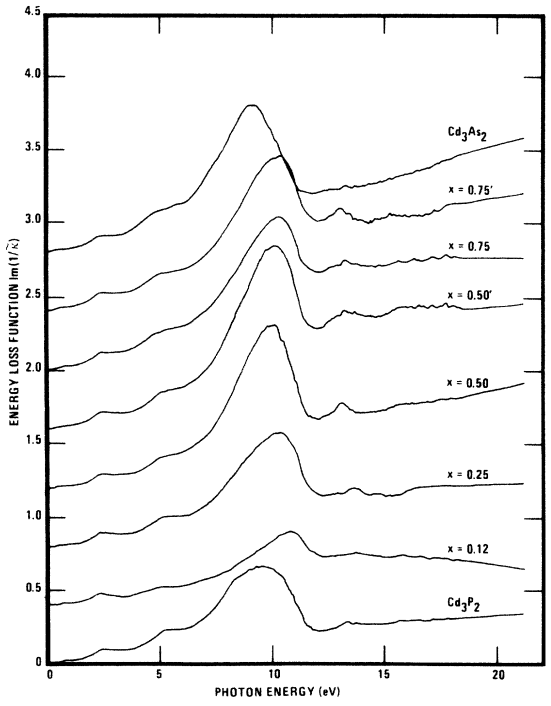

FIG. 13. Characteristic energy-loss function as derived from the dielectric constants (the curves are successively zero shifted in the amount of 0.4 units).

to reach a higher level; however, the absolute reflectance data of this sample has been found to be inconsistent with our Kramers-Kronig extrapolation scheme.

The f-sum rule for interband transitions which involve the valence bands is nearly exhausted in the range of 9 eV. This remark is complimented by these curves of n_{eff}. It is also usually the case that these valence electrons, in conjunction with d-band contributions are able to participate in bulk plasmons. Figure 13 in fact shows a broad peak in the characteristic-energy-loss function $\text{Im}(1/\kappa)$. If the absolute values of our primary data indeed drop too fast in this photon-energy range, then these peaks provide a lower estimate of ~9.5 eV for the plasmon energy. For comparison, the free-electron plasmon energy, due to the valence electrons only is 13.13 eV for Cd_3As_2. This latter number is given for crude comparison only. The d bands not only enhance the effective number of electrons available to contribute to a plasmon, but also provide a measure of shielding

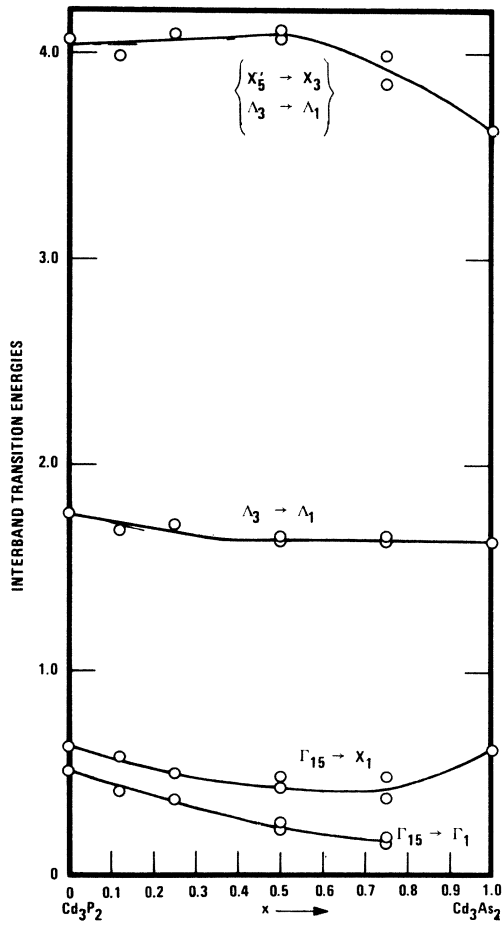

FIG. 14. Probable assignments of direct transitions in the $Cd_3(As_x P_{1-x})_2$ alloy system.

of the Coulomb interactions. Furthermore, the dependence of the plasmon energy on the volume of the unit cells is weak ($E_p \sim V^{-1/2}$). Since the unit-cell volume change from Cd_3As_2 to Cd_3P_2 is small, we do not list the free-electron plasmon energies for the other alloys.

A partial summary of our results is presented in the form of a plot of the structure in κ_2 or R versus the alloy composition. We present these findings in Fig. 14. The upper two curves have been obtained from the peaks in the reflectance data; the lower two curves, from the structure in κ_2.

ACKNOWLEDGMENTS

We wish to acknowledge the assistance of H. W. Ellis and S. P. Zehner in making the extreme-uv measurements and of those for operating the electron storage ring. Helpful discussions and comments from T. C. Collins, F. C. Brown, G. W. Rubloff, and B. Sonntag are gratefully acknowledged. The efforts of E. M. Swiggard of NRL in growing the crystals and the discussions with E. D. Palik and P. J. Lin-Chung have been most valuable.

---

*Research sponsored by the Air Force Office of Scientific Research, Air Force Systems Command, USAF, under Grant No. AFOSR-70-1892. The synchrotron Radiation Facility at the University of Wisconsin is supported under Air Force Contract No. F44620-70-0029.

[1]T. S. Moss, Proc. Phys. Soc. Lond B63, 167 (1950).
[2]W. J. Turner, A. S. Fischler, and W. E. Reese, Phys. Rev. 121, 759 (1961).
[3]W. J. Turner, A. S. Fischler, and W. E. Reese, J. Appl. Phys. Suppl. 32, 2241 (1961).
[4]G. Haacke and G. A. Castellion, J. Appl. Phys. 35, 2484 (1964).
[5]W. Zdanowicz and A. Wojakowski, Phys. Status Solidi 8, 569 (1965).
[6]Y. A. Ugai and T. A. Zyubina, Izv. Akad. Nauk SSSR Neorg. Mater. 1, 860 (1965) [Inorg. Mater. 1, 790 (1965)].
[7]D. P. Spitzer, G. A. Castellion, and G. Haacke, J. Appl. Phys. 37, 3795 (1966), see Appendix.
[8]E. D. Haidemenaksi, M. Balkanski, E. D. Pakik, and J. Tavernier, J. Phys. Soc. Jap. Suppl. 21, 189 (1966).
[9]N. Sexter, Phys. Status Solidi 21, 225 (1967).
[10]L. Zdanowicz, Phys. Status Solidi 20, 473 (1967).
[11]D. Armitage and H. J. Goldsmid, Phys. Lett. A 28, 149 (1968).
[12]F. A. P. Blom and J. T. Schrama, Phys. Lett. A 30, 245 (1969).
[13]I. Rosenman, J. Phys. Chem. Solids 30, 1385 (1969).
[14]S. G. Bishop, W. J. Moore, and E. M. Swiggard, in *Proceedings of the Third International Conference on Photoconductivity, Stanford University, 1969*, edited by F. M. Pell (Pergamon, Oxford, 1971), p. 205.
[15]S. G. Bishop, W. J. Moore, E. M. Swiggard, Appl. Phys. Lett. 16, 459 (1970).
[16]M. W. Heller, J. Babiskin, and P. L. Radoff, Phys. Lett. A 36, 363 (1971).
[17]R. J. Wagner, E. D. Palik, and E. M. Swiggard, Phys. Lett. A 30, 175 (1969).
[18]L. M. Rogers, R. M. Jenkins, and A. J. Crocker, J. Phys. D 4, 793 (1971), see Appendices.
[19]K. Masumoto and S. Isomura, Energy Convers. 10, 129 (1970).
[20]R. J. Wagner, E. D. Palik, and E. M. Swiggard, J. Phys. Chem. Solids Suppl. 1, 471 (1971).
[21]S. G. Bishop and P. L. Radoff, Solid State Commun. 9, 133 (1971).
[22]P. L. Radoff and S. G. Bishop, Phys. Rev. B 5, 442 (1972).
[23]W. Zdanowicz, F. Krolicki, and P. Plenkiewicz, Acta Phys. Pol. A 41, 27 (1972).
[24]J. C. Phillips, Solid State Phys. 18, 55 (1966).
[25]P. J. Lin-Chung, Phys. Rev. 188, 1272 (1969).
[26]P. J. Lin-Chung, Phys. Status Solidi 47, 33 (1971).
[27]V. V. Sobolev, N. N. Syrbu, and S. D. Shutov, *Chemical Bonds in Semiconductors and Thermodynamics*, edited by N. N. Sirota (Consultants Bureau, New York, 1968), p. 165.
[28]M. Zivitz, R. J. Bartlett, and J. R. Stevenson, Bull. Am. Phys. Soc. 15, 1343 (1970).
[29]V. V. Sobolev, N. N. Syrbu, T. A. Zyubina, and Y. A. Ugai, Fiz. Tekh. Poluprovodn. 5, 327 (1971) [Sov. Phys.—Semicond. 5, 279 (1971)].
[30]J. R. Stevenson, M. Zivitz, H. Ellis, and R. J. Bartlett, in the Third International Conference on Vacuum Ultraviolet Radiation Physics, Tokyo, Japan, 1971 (unpublished).
[31]E. M. Rowe, R. A. Otte, C. H. Pruett, and J. D. Steben, IEEE Trans. Nucl. Sci. NS-16, 159 (1969).
[32]W. Zdanowicz, K. Lukaszewicz, and W. Trzebiatowski, Bull. Acad. Pol. Sci. Ser. Sci. Chim. 12, 169 (1964).
[33]M. V. Stackelberg and R. Paulus, Z. Phys. Chem. B28, 427 (1935).
[34]G. A. Steigmann and J. Goodyear, Acta Crystallogr. B 24, 1062 (1968).
[35]J. C. Slater, Phys. Rev. 98, 1039 (1955).
[36]H. Harrison, J. Chem. Phys. 901 (1970).
[37]C. E. Moore, *Atomic Energy Levels*, Natl. Bur. Std. Circ. No. 35 (U.S. GPO, Washington, D. C., 1971), Vols. 1–3.
[38]J. P. Suchet, J. Phys. Chem. Solids 16, 265 (1960).
[39]W. A. Harrison, *Solid State Theory* (McGraw-Hill, New York, 1970).
[40]M. Zivitz, Ph.D. Thesis (Georgia Institute of Technology, 1973) (unpublished).
[41]P. D. Johnson, J. Opt. Soc. Am. 42, 278 (1952).
[42]D. C. Hinson, Ph.D. Thesis (Georgia Institute of Technology, 1967) (unpublished).
[43]R. A. Smith, *Semiconductors* (Cambridge U. P., Cambridge, U. K., 1968), general reference.
[44]E. D. Palik and E. M. Swiggard (private communication).
[45]E. O. Kane, J. Phys. Chem. Solids 1, 249 (1957).

[46]H. Ehrenreich, J. Appl. Phys. Suppl. 32, 2155 (1961).
[47]F. Herman, C. D. Kuglin, K. F. Cuff, and R. L. Kortum, Phys. Rev. Lett. 11, 541 (1963).
[48]M. L. Cohen and T. K. Bergstresser, Phys. Rev. 141, 789 (1966).
[49]H. R. Philipp and H. Ehrenreich, Phys. Rev. 129, 1550 (1963).
[50]J. L. Freeouf, Phys. Rev. B 7, 3810 (1973).
[51]R. J. Bartlett, D. W. Lynch, and R. Rosei, Phys. Rev. B 3, 4074 (1971).
[52]F. Stern, Solid State Phys. 15, 299 (1963).
[53]J. L. Shay (private communication).
[54]D. L. Greenaway and G. Harbeke, *Optical Properties and Band Structure of Semiconductors* (Pergamon Press, Oxford, 1968).
[55]M. Cardona, Phys. Rev. 129, 69 (1963).